SPANDIDOS PUBLICATIONS

ONCOLOGY REPORTS 42: 1237-1247, 2019

Inhibition of ubiquitin-specific protease 14 promotes connexin 32 internalization and counteracts cisplatin cytotoxicity in human ovarian cancer cells

HUIMIN LUO[1*], XIYAN WANG[2*], HUI GE[2], NINGZE ZHENG[1], FUHUA PENG[1], YILE FU[1], LIANG TAO[1,2] and QIN WANG[1]

[1]Department of Pharmacology, Zhongshan School of Medicine, Sun Yat-Sen University, Guangzhou, Guangdong 510080; [2]Tumor Research Institute, Xinjiang Medical University Affiliated Tumor Hospital and State Key Laboratory Jointly Established by The Province and Ministry, Urumqi, Xinjiang Uygur Autonomous Region 830000, P.R. China

Received March 10, 2019; Accepted July 3, 2019

DOI: 10.3892/or.2019.7232

Abstract. Although cisplatin is one of the most accepted therapies for ovarian cancer, recurrence and drug resistance remain problematic. Both the ubiquitin-proteasome system (UPS) and connexin (Cx) are closely related to tumor progression. However, the role of ubiquitin-specific protease 14 (USP14) and Cx in mediating drug resistance remains unclear. In the present study, we aimed to determine whether USP14 is involved in cisplatin resistance and modulates the internalization of connexin 32 (Cx32) in ovarian cancer. The results of the deubiquitinase (DUB) trap assay and western blot analysis revealed that the expression and activity levels of USP14 were downregulated in A2780 cisplatin-resistant cells (A2780-CDDP) relative to these levels in A2780 cisplatin-sensitive cells (A2780). CCK-8 assay results showed that inhibition of USP14 by a specific inhibitor or siRNA decreased cisplatin cytotoxicity in A2780 cells. Additionally, USP14 inhibition increased the expression of Cx32 without changing its mRNA and ubiquitination levels, as showed by Real-time qPCR and immunoprecipitation assay respectively. Cisplatin resistance induced by USP14 inhibition was counteracted by Cx32 knockdown. Moreover, USP14 inhibition contributed to Cx32 internalization, as determined by western blot analysis and a reduction in gap junction intercellular communication (GJIC), as showed by parachute dye-coupling assay. Collectively, these data suggest that Cx32 internalization by USP14 inhibition modulates the cisplatin resistance in ovarian cancer cells, thus serving as a potential drug target to challenge chemotherapy failure. In addition, USP14 can also be used as a marker to monitor the development of cisplatin resistance in ovarian cancer treatment.

Correspondence to: Professor Liang Tao or Professor Qin Wang, Department of Pharmacology, Zhongshan School of Medicine, Sun Yat-Sen University, 74 Zhongshan 2nd Road, Guangzhou, Guangdong 510080, P.R. China
E-mail: taol@mail.sysu.edu.cn
E-mail: wangqin6@mail.sysu.edu.cn

*Contributed equally

Abbreviations: USP14, ubiquitin-specific protease 14; Cx, connexin; Cx32, connexin 32; GJIC, gap junction intercellular communication; UPS, ubiquitin-proteasome system; NEDD4, neural precursor cell-expressed developmentally downregulated gene 4; USP8, ubiquitin-specific protease 8; Cx43, connexin 43; siRNA, small interfering RNA; Eps15, EGF receptor pathway substrate 15; AMSH, associated molecule with the SH3 domain of STAM; Hrs, hepatocyte growth factor-regulated tyrosine kinase substrate; TSG101, tumor susceptibility gene 101; TP53BP1, tumor protein p53 binding protein 1; RNF168, ring finger protein 168; DDR, DNA damage response

Key words: ovarian cancer, cisplatin, cytotoxicity, ubiquitin-specific protease 14, connexin 32, internalization

Introduction

Ovarian cancer is the leading cause of death among all gynecologic malignancies and platinum compounds are the standard first-line agents for the treatment of ovarian cancer (1). However, nearly 75% of patients who are highly responsive to cisplatin treatment experience recurrence within 2 years and fail to respond to available treatments due to acquired resistance (2,3). Therefore, uncovering the mechanisms of cisplatin resistance and seeking new therapeutic targets are critical for prolonging the survival of patients.

Gap junctions (GJs) are composed of two hemichannels, each of which consists of six connexin (Cx) monomers, enabling the electrical coupling and sharing of ions and signaling molecules (4). Almost all tissues and cells are affected by this communication junction. Defective gap junction intercellular communication (GJIC) has been observed in carcinogenic progression. A lager number of studies have proved that GJs and Cx are potential targets for tumor therapy (5,6).

However, emerging evidence has been found in recent years showing that the increased expression of Cx may lead to tumors with more aggressive phenotypes (7,8). The cytoplasmic distribution of Cx also exerts an advantageous effect on tumor progression. Kawasaki *et al* and Li *et al* reported that cytoplasmic accumulation of Cx32 expanded the cancer stem cell population and enhanced the motility and metastatic ability of human hepatoma cells (9,10). Studies performed by our team demonstrated that upregulated Cx32 in cervical ovarian and liver cancer cells was mainly localized in the cytoplasm and produced anti-apoptotic and pro-tumor effects in a GJ-independent manner (11-14). Nevertheless, the mechanism of the upregulation and internalization of Cx32 remains unknown.

The ubiquitin-proteasome system (UPS) is an important pathway for the degradation of unnecessary proteins and maintenance of protein homeostasis. This system comprises the 26S proteasome and a sequence of enzymes (E1, E2 and E3) capable of activating ubiquitin residues and adding them to the target protein (15,16). In contrast, deubiquitinases (DUBs) remove ubiquitin (Ub) chains from the target protein prior to degradation. It has been reported that ubiquitination is involved in the life cycle and localization of Cx (17,18). E3 ubiquitin ligase neural precursor cell-expressed developmentally down-regulated gene 4 (NEDD4) catalyzed the ubiquitination and endocytosis of Cx43, which decreased GJIC (19,20). Sun *et al* showed that ubiquitin-specific protease 8 (USP8) reduced both multiple monoubiquitination and polyubiquitination of Cx43 to prevent autophagy-mediated degradation (21). However, these studies mostly focused on Cx43, and little research has been performed in regards to Cx32.

Ubiquitin-specific protease 14 (USP14) is one of the three DUBs associated with the 19S regulatory particle in mammalian cells. USP14 disassembles the ubiquitin chain from its substrate-distal tip and serves as a quality control component to rescue proteins from degradation (22). Upregulation of USP14 is involved in the progression of non-small cell lung cancer (23), breast cancer (24), ovarian cancer (25) and gastric cancer (26). USP14 knockdown was found to suppress the proliferation and induced apoptosis of cancer cells. Therefore, USP14 is proposed to be a target for cancer therapy. Furthermore, many studies have shown that ubiquitination is closely related to chemotherapy resistance (27-29). However, the role of USP14 in acquired cisplatin resistance of ovarian cancer remains unrevealed. Kaplan-Meier analysis demonstrated that the low expression of USP14 in ovarian cancer patients predicts poorer progression-free survival (PFS) (Fig. 1A). Whether USP14 is related with acquired cisplatin resistance and Cx32 internalization in ovarian cancer is unclear.

In the present study, lower expression and activity of USP14 was found in ovarian cancer A2780-CDDP (cisplatin-resistant) cells when compared with these parameters in A2780 (cisplatin-sensitive) cells. USP14 inhibition induced cisplatin resistance in A2780 cells. In addition, USP14 inhibition upregulated Cx32 expression without changing the levels of Cx32 mRNA and ubiquitination. Cisplatin insensitivity by USP14 inhibition was abrogated when Cx32 expression was knocked down in A2780 cells. Furthermore, upregulated Cx32 protein was internalized, and GJIC was decreased. In conclusion, the present study revealed that USP14 inhibition modulated Cx32 localization and decreased cisplatin sensitivity in ovarian cancer cells, indicating that Cx32 internalization regulated by USP14 may serve as a marker of chemosensitivity.

Materials and methods

Analysis of Kaplan-Meier survival tool. The Kaplan-Meier Plotter (http://kmplot.com/analysis/) was used to analyze the association between USP14 expression and progression-free survival (PFS) of patients with ovarian cancer. The following datasets were used for the analysis: GSE14764 (30), GSE15622 (31), GSE18520 (32), GSE19829 (33), GSE23554 (34), GSE26193 (35,36), GSE26712 (37,38), GSE27651 (39), GSE30161 (40), GSE3149 (41), GSE51373 (42), GSE63885 (43), GSE65986 (44), GSE9891 (45) and TCGA. 'USP14' was input in Affy id/Gene symbol and chose 'Affy ID: 201671_x_at'. The median expression level of USP14 mRNA was regarded as the dividing line and 1435 patients were divided into low expression group and high expression group. Other parameters remain unchanged by default and draw Kaplan-Meier plot. P-values <0.05 were considered to indicate a statistically significant result.

Reagents. Cisplatin (cat. no. P4394) was obtained from Sigma-Aldrich; Merck KGaA. IU1 [1-[1-(4-fluorophenyl)-2,5-dimethylpyrrol-3-yl]-2-pyrrolidin-1-ylethanone] (cat. no. S7134) (a specific small-molecule inhibitor of USP14) was purchased from Selleck Chemicals (Houston, TX, USA).

Antibodies. The mouse monoclonal anti-Cx32 (cat. no. 59948) antibody was purchased from Santa Cruz Biotechnology, Inc. (Dallas, Texas, USA). The mouse monoclonal anti-β-tubulin (cat. no. 86298), mouse monoclonal anti-β-actin (cat. no. 3700), rabbit monoclonal anti-USP14 (cat. no. 11931), rabbit monoclonal anti-caspase-3 (cat. no. 9662), rabbit monoclonal anti-cleaved caspase-3 (cat. no. 9664), rabbit anti-caspase-9 (cat. no. 9502), rabbit anti-Na,K-ATPase (cat. no. 3010) and mouse monoclonal IgG1 (cat. no. 5415S) antibodies were purchased from Cell Signaling Technology, Inc. (Danvers, MA, USA). Peroxidase-AffiniPure goat anti-mouse IgG (H+L) (cat. no. 115-035-003) and Peroxidase-AffiniPure goat anti-rabbit IgG (H+L) (cat. no. 111-035-003) were obtained from Jackson (West Grove, PA, USA). The rabbit monoclonal anti-ubiquitin (cat. no. EPR8830) was purchased from Abcam (Cambridge, UK). The secondary antibody IPKine HRP, mouse anti-rabbit IgG LCS (cat. no. A25002) was purchased from Abbkine Scientific Co., Ltd. (Wuhan, China).

Cell lines and cell culture. A2780 cisplatin-sensitive cells (A2780) were obtained from the American Type Culture Collection (ATCC; Manassas, VA, USA). The A2780 cisplatin-resistant cells (A2780-CDDP) were established by a previously described method (11). Both A2780 and A2780-CDDP cell lines were cultured in Dulbecco's modified Eagle's medium (DMEM) (cat. no. 12800017; Gibco; Thermo Fisher Scientific, Inc.) containing 10% fetal bovine serum (FBS) (Gibco; Thermo Fisher Scientific, Inc.) and 1% penicillin/streptomycin at 37˚C in an atmosphere containing 5% CO_2.

siRNA and shRNA transfection experiments. After growing A2780 cells to 30-50% confluence, 50 nM of non-specific siRNA (#siN0000001-1-5) and siRNAs targeting the human USP14 gene were transfected into cells with Lipofectamine 3000 transfection reagent (cat. no. L3000015; Invitrogen; Thermo Fisher Scientific, Inc.) according to the manufacturer's protocol. The sequences of the synthesized siRNAs targeting USP14 (Guangzhou RiboBio, Co., Ltd., Guangzhou, China) were as follows: siUSP14-1, 5'-CTGGCA TATCGCTTACGTT-3'; siUSP14-2, 5'-TCCAGTATTCCA CCTATTA-3'; and siUSP14-3: 5'-TTGCCGAGAAAGGTG AACA-3'.

To generate stably transfected cells, A2780 cells were transfected with lentiviral plasmids containing the shCx32 sequence or with the negative control vector (pLVX-shRNA-tdTomato-Puro), which were constructed by Landbiology, Co., Ltd. (Guangzhou, Guangdong, China). Lentiviral particles were prepared by transfecting 293T cells with the lentiviral plasmids, PAX2 and pMD2.G at a defined ratio. A2780 cells were incubated with medium containing the virus and Polybrene for 48 h. After infection, cells were selected by culturing with puromycin (2 μg/ml) for 2 weeks. The sequences of the short hairpin RNA targeting Cx32 (shCx32) were as follows: 5'-GCTGCAACAGCGTTTGCTACTCGA GTAGCAAACGCTGTTGCAGCTTTTTTT-3'. shRNA with non-specific sequences (5'-TTCTCCGAACGTGTCACGTTT CTCGAGAAACGTGACACGTTCGGAGAA-3') was used as the control scrambled RNA.

Cell viability assay. Cell Counting Kit-8 (CCK-8) (Dojindo Molecular Technologies Inc., Kumamoto, Japan) was used to examine cell viability according to the manufacturer's instructions. Cells were seeded in 96-well plates at a suitable density of 5,000 cells/well. Then, siUSP14-1 was added for 24 h and the cells were treated with cisplatin for 48 h or the cells were cotreated with IU1 and cisplatin for 48 h. CCK-8 solution diluted with FBS-free DMEM at a ratio of 1:9 was added in a total volume of 100 μl. The 96-well plates were incubated at 37˚C for 1-2 h. The optical density (OD) was determined at 450 nm using an Epoch microplate spectrophotometer (BioTek; Winooski, VT, USA). The concentration of cisplatin resulting in 50% growth inhibition (IC_{50}) was calculated using GraphPad Prism 6.0 software (GraphPad Software, Inc.).

Western blot analysis. Cells were lysed at 4˚C in buffer [1 mM β-glycerophosphate, 2.5 mM sodium pyrophosphate, 20 mM Tris-HCl (pH 7.4), 1% Triton X-100, 150 mM NaCl, 1 mM EGTA, 1 mM EDTA and 1 mM Na_3VO_4] supplemented with protease inhibitor cocktail (cat. no. P8340; Merck KGaA) (1:1,000). After ultrasonication, cell lysates were cleared at 12,000 x g for 30 min at 4˚C. The protein concentration was determined with a BCA protein assay kit (Thermo Fisher Scientific, Inc.). A total of 20 μg of protein from each sample was separated using SDS-PAGE and transferred to PVDF membranes. Membranes were blocked with 5% (w/v) skim milk in wash buffer TSBT (TBS and 0.05% Tween-20) for 1 h and were then incubated with specific antibodies against Cx32 (dilution 1:2,000), USP14 (dilution 1:1,000), cleaved caspase-3 (dilution 1:1,000), caspase-3 (dilution 1:1,000), caspase-9 (dilution 1:1,000), Na,K-ATPase (dilution 1:1,000), β-actin (dilution 1:10,000) and β-tubulin (dilution 1:10,000) overnight at 4˚C. After being washed for three times with TBST, membranes were incubated with HRP-conjugated secondary antibodies (dilution 1:10,000) for 2 h at room temperature. The membranes were then washed with TBST before being visualized using a Chemiluminescent HRP Substrate Kit (Millipore; Billerica, MA, USA) and scanned using an ImageQuant LAS 4000™ (GE Healthcare). β-tubulin and β-actin were used as loading control, and band densities were quantified using ImageJ software (NIH, National Institutes of Health, Bethesda, MD, USA).

DUB trap assay. DUB activity can be inhibited irreversibly using ubiquitin-vinylsulfone (Ub-VS), which forms an adduct with the active site cysteine in DUB of the thiol protease class (22). Cells were lysed via mild sonication in ice-cold buffer containing 50 mM Tris (pH 7.4), 5 mM $MgCl_2$, 250 mM sucrose, 1 mM DTT, 2 mM ATP and 1 mM PMSF. Lysates were cleared by centrifugation at 12,000 x g for 30 min at 4˚C, and 30 μg of protein extract was incubated for 15 min at 37˚C with 1 μM HA-Ub-VS (cat. no. U-212; Boston Biochem, Cambridge, MA, USA). After boiling in loading buffer, labeled cell lysates were subjected to immunoblot analysis. After transferring to PVDF membranes, HA-Ub-VS labeled USP14 was immunodetected using the USP14 antibody. The probe group was a blank control and β-actin was used as a loading control. The band densities of USP14-Ub-VS were quantification for the activity of USP14 (46).

Flow cytometry apoptosis detection assay. A2780 cells were seeded in 6-well plates and incubated with IU1 (50 μM), cisplatin (8 μg/ml) or cotreated with IU1 (50 μM) and cisplatin (8 μg/ml) for 48 h. Afterward, the cells were trypsinized and washed twice with cold PBS. After the cells were re-suspended in binding buffer, Annexin V-FITC and propidium iodide (PI) (cat. no. KGA105-KGA108; Keygen; Nanjing, Jiangsu, China) were used to stain cells for 15 min away from light at room temperature. Subsequently, the cells were immediately analyzed with FACScan (Beckman Instruments, Fullerton, CA, USA) and cell apoptosis was analyzed using FlowJo 7.6 software (FlowJo LLC, Ashland, OR, USA).

Real-time qPCR assay. Approximately $1.5x10^5$ A2780 cells were seeded into 6-well plates. After adherence, the cells were incubated with IU1 or siUSP14-1 for 48 h. Total RNA was extracted using TRIzol (cat. no. A33252; Invitrogen; Thermo Fisher Scientific, Inc.) according to the manufacturer's instructions. The concentration of RNA was measured by NanoDrop 2000 Spectrophotometer (Thermo Fisher Scientific, Inc.). Then 1 μg total RNA was reverse transcribed using a Transcriptor cDNA Synthesis kit (cat. no. 4896866001; Roche; Basel, Switzerland) by C1000 Thermal Cycler (Bio-Rad Laboratories, Inc.; Hercules, CA, USA). The resulting cDNA was subjected to real-time qPCR in a final reaction volume of 20 μl using FastStart Universal SYBR Green Master (Rox) (cat. no. 04913914001; Roche) by the ABI Applied Biosystems StepOne Quantitative Real-Time PCR System (Thermo Fisher Scientific, Inc.). The thermocycling conditions were as follows: 10 min at 95˚C, followed by denaturation at 95˚C for 15 sec; annealing and extension

at 60˚C for 60 sec. Primers were as follows: USP14 (forward, 5'-GGCTTCAGCGCAGTATATTA-3' and reverse, 5'-CAG ATGAGGAGTCTGTCTCT-3'); Cx32 (forward, 5'-ACA CCTTGCTCAGTGGCGTGA-3' and reverse, 5'-GGGACC ACAGCCGCACATGG-3'); and GAPDH (forward, 5'-GGA GCGAGATCCCTCCAAAAT-3' and reverse, 5'-GGCTGT TGTCATACTTCTCATGG-3'). The analysis for USP14 and normalization control gene GAPDH was performed according to the $2^{-\Delta\Delta q}$ method (47).

Immunoprecipitation. A2780 cells were treated with IU1 (50 μM for 48 h) and then incubated with 10 μM MG132 (cat. no. S2619; Selleck Chemicals) for 4 h prior to harvesting in buffer [1 mM β-glycerophosphate, 2.5 mM sodium pyrophosphate, 20 mM Tris-HCl (pH 7.4), 1% Triton X-100, 150 mM NaCl, 1 mM EGTA, 1 mM EDTA and 1 mM Na_3VO_4] supplemented with protease inhibitor cocktail (1:1,000). The samples were then centrifuged at 12,000 x g for 30 min, and the supernatants were used for immunoprecipitation. Briefly, 1-2 μl of mouse monoclonal anti-Cx32 was added to 500-1,000 μg of protein and incubated for 3 h at 4˚C. Non-specific antibodies were used as controls. Then, 20 μl of Protein G plus/Protein A agarose suspension (cat. no. IP05; Merck KGaA) was added to the mixture. Following incubation for more than 12 h at 4˚C, the samples were centrifuged at 12,000 x g for 3 min, and the protein G-Sepharose precipitate was washed 5 times in an appropriate wash buffer (500 mM NaCl, 50 mM Tris-HCl, 6 mM EDTA and 1% Triton X-100, pH 8.3), resuspended in 4X loading buffer, and denatured at 100˚C for 5 min. The input represented 10% of the total amount of protein in the lysates before immunoprecipitation. All samples were subjected to immunoblot analysis. After separation by SDS-PAGE, the proteins samples were transferred to PVDF membrane. Membranes were blocked with 5% (w/v) skim milk in wash buffer (TBS and 0.05% Tween-20) for 1 h and were then incubated with specific antibodies against ubiquitin (dilution 1:1,000). The secondary antibody IPKine HRP, mouse anti-rabbit IgG LCS (dilution 1:5,000) was used to incubated the membrane for eliminating heavy chain interference.

Parachute dye-coupling assay. GJIC was evaluated by a 'parachute' dye coupling assay, as described by Goldberg *et al* (48) and Koreen *et al* (49). Calcein-AM (cat. no. C3100MP) and CM-DiI (cat. no. C3100MP) were purchased from Invitrogen (Thermo Fisher Scientific, Inc.). Cells were seeded in 12-well plates at an appropriate density of 50,000 cells/well. After confluence, the donor cells were labeled with both Calcein-AM (green fluorescence, GJ permeable) and CM-DiI (red fluorescence, non-permeable) at 37˚C for 30 min. After being rinsed and trypsinized, 500 donor cells were seeded onto the receiver cells per well and incubated at 37˚C for 4-6 h. Signal intensity was observed using a fluorescence microscope (Olympus IX71; Tokyo, Japan). The average number of receiver cells (green fluorescence) around every donor cell (both green and red fluorescence) was recorded as an index of GJIC.

Membrane protein extraction. Approximately 2-3x10^6 A2780 cells were seeded in a 10-cm culture dish. IU1 or siUSP14-1 was administered for 48 h when the confluence was 30-40%. Membrane-bound and cytoplasmic proteins were extracted by using a ProteoExtract Transmembrane Protein Extraction Kit (cat. no. 71772; Merck KGaA) according to the manufacturer's instructions. Cells were collected in PBS and centrifuged at 1,000 x g for 5 min at 4˚C. Cells were resuspended in Extraction Buffer 1 containing protease inhibitor cocktail and incubated for 10 min at 4˚C. The cytosolic (soluble) protein fraction was harvested after centrifugation at 1,000 x g for 5 min at 4˚C. The pellet was resuspended in Extraction Buffer 2 containing TM-PEK reagent B and protease inhibitor cocktail. The mixture was incubated for 45 min at 4˚C with gentle agitation, and membrane proteins were obtained in the supernatant.

Statistical analysis. Every *in vitro* experiment was performed with a minimum of three independent cell cultures. The data were statistically analyzed by Student's t-test (2 groups), one-way ANOVA (>2 groups), followed by Tukey's multiple comparison test or two-way ANOVA (>2 groups), followed by Bonferroni post test with GraphPad Prism 6.0 software. Histograms or scatter diagrams were constructed with the GraphPad Prism 6.0 software (GraphPad Software, Inc.). The results are expressed as the mean ± SE, and $P<0.05$ was considered indicative of statistical significance.

Results

The decreased USP14 expression predicts poor prognosis in ovarian cancer. A cohort of 1435 cases of ovarian cancer of following datasets were used for Kaplan-Meier analysis: GSE14764 (30), GSE15622 (31), GSE18520 (32), GSE19829 (33), GSE23554 (34), GSE26193 (35,36), GSE26712 (37,38), GSE27651 (39), GSE30161 (40), GSE3149 (41), GSE51373 (42), GSE63885 (43), GSE65986 (44), GSE9891 (45) and TCGA. The results showed that decreased USP14 expression is associated with poorer progression-free survival (PFS) of patients with ovarian cancer ($P<0.001$; Fig. 1A). Then we performed experiments to explore the role of USP14 in cisplatin resistance of ovarian cancer.

Activity and expression of USP14 were decreased in A2780-CDDP cells. The A2780-CDDP cells were established by a previously described method (11). The IC_{50} of the A2780 cells used in present study was 5.946±0.61 μg/ml, and the IC_{50} of the A2780-CDDP cells was 32.45±2.52 μg/ml. The resistance index (RI) was 5.46. A2780-CDDP cells were moderately resistant to cisplatin and qualified for subsequent experiments (Fig. 1B). As showed in Fig. 1C, the expression of Cx32 was significantly higher while the expression of USP14 was significantly lower in the A2780-CDDP cells when compared to the expression levels in A2780 cells. Furthermore, the results of DUB trap assay showed that USP14 activity was significantly decreased in the A2780-CDDP cells (Fig. 1D).

Inhibition of USP14 in A2780 cells decreases cisplatin cytotoxicity. Next we sought to determine whether USP14 is involved in cisplatin resistance. It has been reported that IU1 specifically inhibits USP14 by preventing its docking on the proteasome (22). Therefore IU1 was used as a USP14 inhibitor. A2780 cells were incubated with gradient concentrations

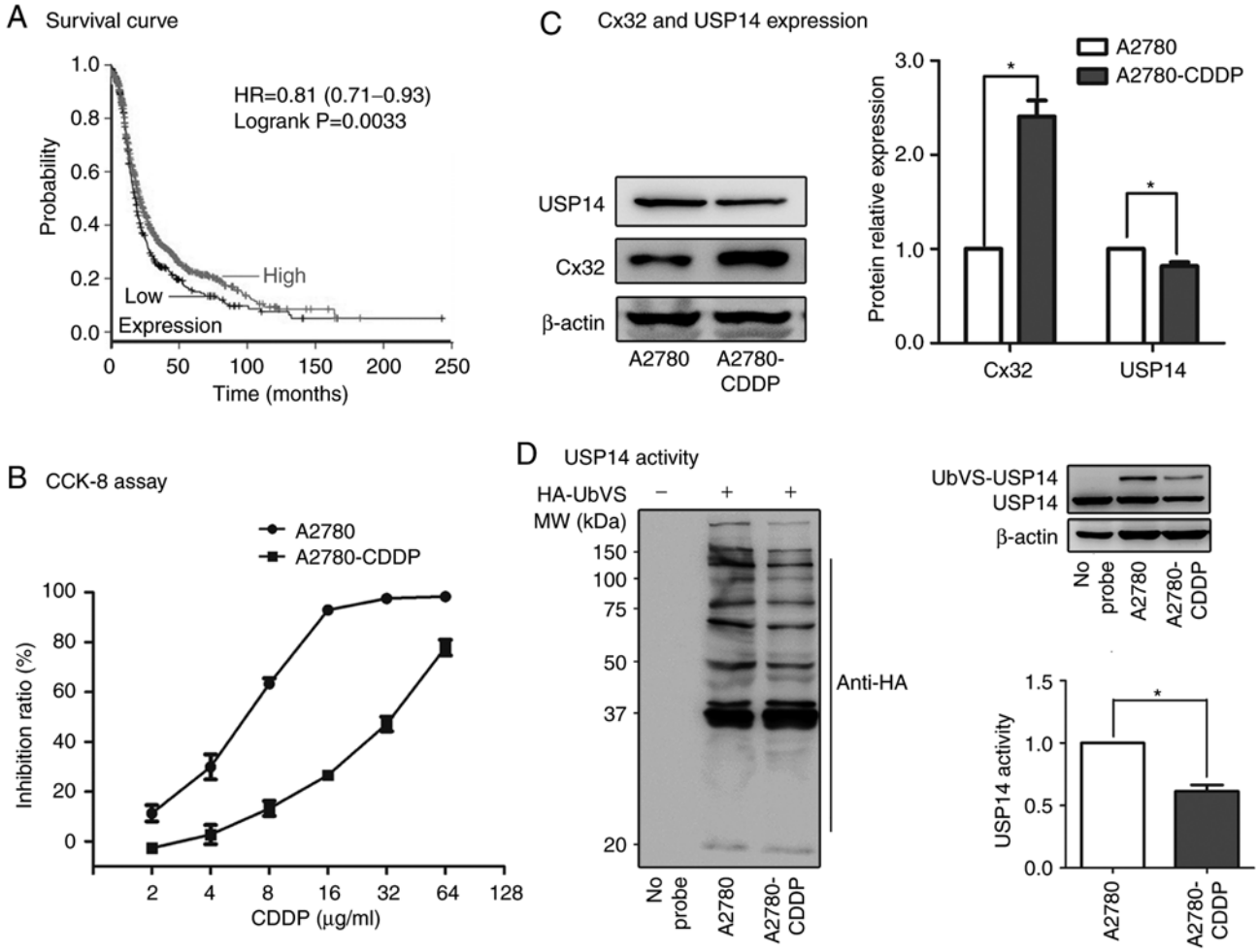

Figure 1. Low expression and activity of USP14 in A2780-CDDP cells. (A) Kaplan-Meier analysis indicates that low USP14 expression is associated with poorer progression-free survival (PFS) of patients with ovarian cancer (http://kmplot.com/analysis/). (http://kmplot.com/analysis/index.php?p=background). (B) The IC_{50} value of cisplatin (CDDP) was determined by a CCK-8 assay in A2780 and A2780-CDDP cells. The RI was 5.46, and the cells were suitable for subsequent study. (C) The Cx32 expression level was significantly increased while the USP14 expression level was significantly decreased in the A2780-CDDP cells relative to these levels in the A2780 cells. (D) The band on the left was incubated with anti-HA antibody to verify the reliability of the DUB trap assay. The bands and graph on the right show that the activity of USP14 was consistently downregulated in the A2780-CDDP cells compared to that in A2780 cells. The results are presented as the mean ± SE. *P<0.05. n=3. HR, hazard ratio; USP14, ubiquitin-specific protease 14; Cx32, connexin 32.

(5, 10, 25, 50 and 100 μM) of IU1 for 48 h. The results of CCK-8 assay indicated that 100 μM IU1 significantly inhibited A2780 cell proliferation while 0-50 μM IU1 had no effect (Fig. 2A). Hence, we chose 50 μM IU1 for subsequent studies. As expected, 50 μM IU1 clearly inhibited the activity of USP14 in A2780 cells without changing its protein level (Fig. 2B). The results of CCK-8 assay revealed that IU1 markedly counteracted cisplatin cytotoxicity (Fig. 2C). To make the experiments more convincing, siRNAs were used to inhibit USP14 expression. siUSP14-1 showed the greatest efficiency in silencing USP14 expression (Fig. 2D). Moreover, siUSP14-1 decreased both the protein level and activity of USP14 (Fig. 2E). Then A2780 cells were transfected with siUSP14-1 for 24 h, followed by cisplatin administration for 48 h. Similarly, USP14 knockdown decreased cisplatin cytotoxicity in A2780 cells (Fig. 2F).

Additionally, the apoptosis rate of the cells was examined by flow cytometry, and the levels of cleaved caspase-9 and cleaved caspase-3, two well-known protein markers of apoptosis, were assessed by western blotting. As showed in Fig. 2G-I, significant apoptosis of A2780 cells was induced by cisplatin (8 μg/ml, 48 h) but was significantly suppressed by cotreatment with the USP14 inhibitor IU1 (50 μM, 48 h; Fig. 2G and H) or siUSP14-1 (Fig. 2I). Taken together, these results indicated that USP14 inhibition decreased cisplatin-induced apoptosis.

Inhibition of USP14 increases expression of Cx32 without altering its mRNA and ubiquitination levels. Our previous studies reported that the anti-apoptotic effect of USP14 inhibition was closely related to the upregulation of Cx32 expression in cervical and ovarian cancer (11,13). The present results showed that cisplatin cytotoxicity was also reduced by USP14 inhibition in A2780 cells. Then, we aimed to ascertain whether USP14 inhibition could affect the expression of Cx32. As showed in Fig. 3A and B, IU1 (50 μM, 48 h) and siUSP14-1 alone or in combination with cisplatin upregulated Cx32 expression. To further explore this mechanism, qPCR and immunoprecipitation were performed. The results demonstrated that the mRNA and ubiquitination level of Cx32 remained unchanged. Moreover, the ubiquitination level of Cx32 in A2780 cells was

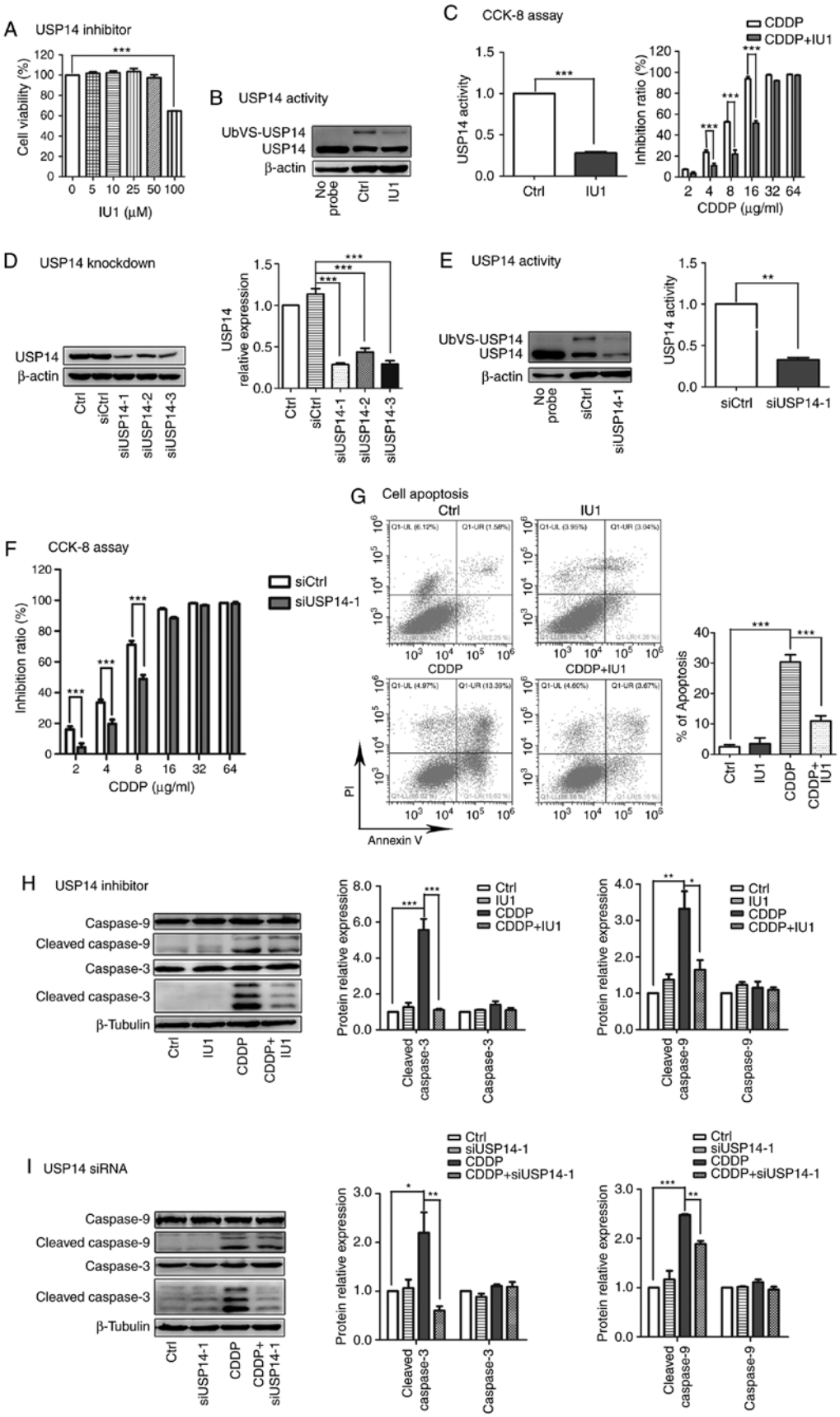

Figure 2. USP14 inhibition counteracts cisplatin cytotoxicity in A2780 cells. (A) A 100 μM concentration of IU1 had significant inhibitory effects on A2780 cell proliferation, while concentration of 0 to 50 μM IU1 did not. (B) IU1 (50 μM) appreciably suppressed USP14 activity. (C) IU1 (50 μM) induced cisplatin insensitivity in A2780 cells. (D) Western blotting verified that USP14 expression was significantly knocked down via siRNA. (E) Both the expression and activity of USP14 were decreased by siUSP14-1. (F) USP14 knockdown reduced cisplatin cytotoxicity. (G) Significant apoptosis of A2780 cells was induced by cisplatin (8 μg/ml, 48 h) but was significantly suppressed following cotreatment with IU1 (50 μM, 48 h). (H and I) Western blot analysis shows that cisplatin (8 μg/ml) induced caspase-3 and caspase-9 cleavage but was significantly suppressed by cotreatment with IU1 (50 μM, 48 h) or siUSP14-1. The levels of caspase-3 and caspase-9 remained unchanged. The results are presented as the mean ± SE. *P<0.05, **P<0.01 and ***P<0.001. n=3. Ctrl, control; USP14, ubiquitin-specific protease 14.

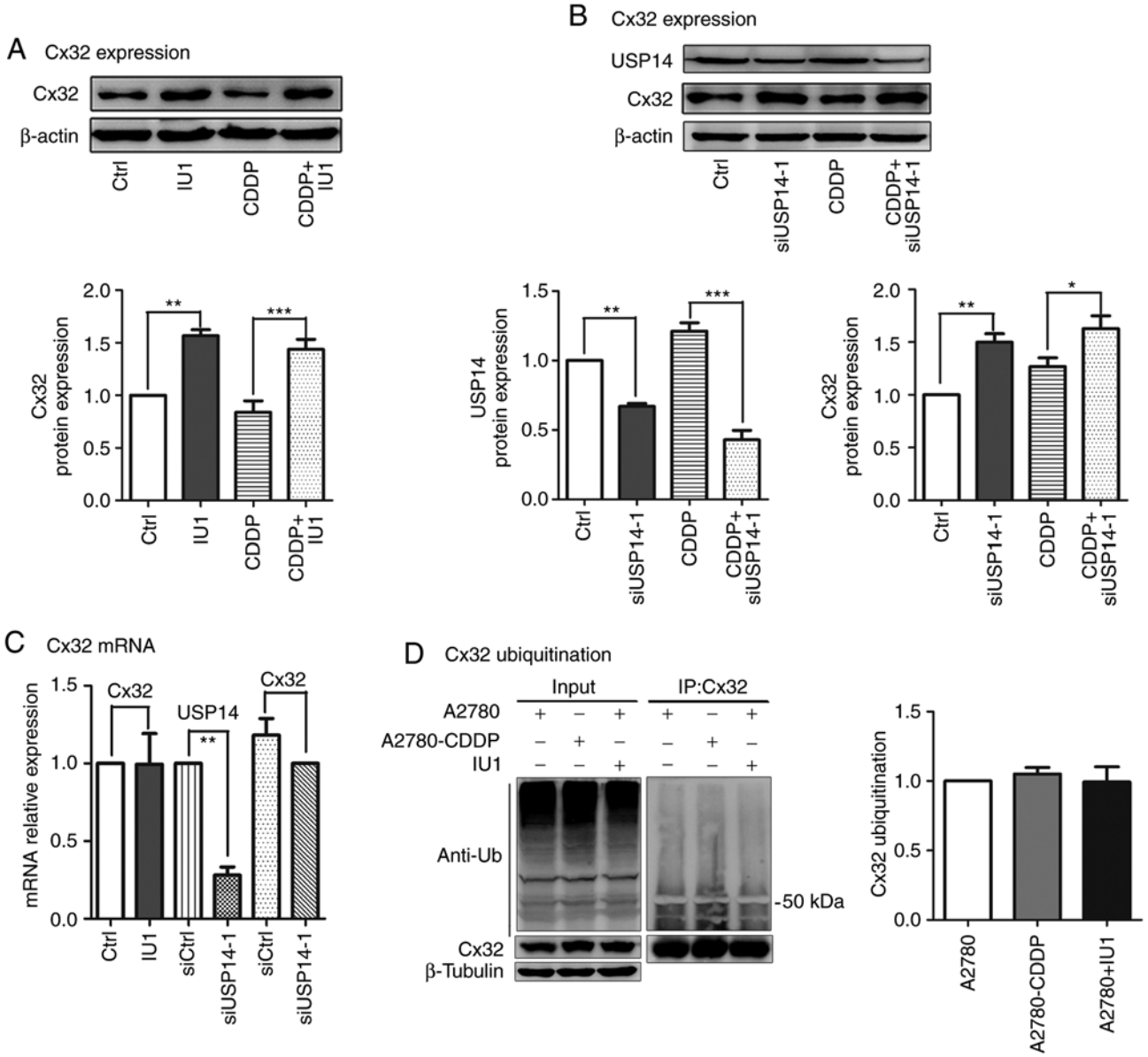

Figure 3. Inhibition of USP14 increases the expression of Cx32 without changing its mRNA and ubiquitination levels. (A) Compared with the control and cisplatin (CDDP) groups, the IU1 and cotreatment groups exhibited upregulated Cx32 protein expression. (B) Compared with the control and cisplatin (CDDP) groups, the siUSP14-1 and cotreatment groups exhibited upregulated Cx32 protein expression. (C) The Cx32 mRNA level was not altered by USP14 inhibition using IU1 and siUSP14-1. (D) USP14 inhibition did not affect the ubiquitination level of Cx32 and there was no significant difference in the ubiquitination level of Cx32 between A2780 and A2780-CDDP cells. The results are presented as the mean ± SE. *P<0.05, **P<0.01 and ***P<0.001. n=3. Ctrl, control; USP14, ubiquitin-specific protease 14; Cx32, connexin 32.

consistent with that in A2780-CDDP cells (Fig. 3C and D). Taken together, USP14 inhibition increased the expression of Cx32 without changing its mRNA and ubiquitination levels.

Cx32 knockdown counteracts USP14 downregulation-induced cisplatin resistance in A2780 cells. The above results showed that IU1 and siUSP14-1 alone or in combination with cisplatin upregulated Cx32 expression. To determine the role of Cx32 in the anti-apoptotic effect of USP14 inhibition, Cx32 expression was knocked down with shRNA in A2780 cells (Fig. 4A). As shown in Fig. 4B, cytotoxicity was increased in the Cx32-knockdown cells compared with that in A2780 cells after administration of 2 or 4 μg/ml cisplatin. Similarly, cytotoxicity was increased in the Cx32-knockdown cells compared with that in A2780 cells after co-administration. Although the anti-apoptotic effect of cotreatment remained after Cx32 knockdown, the extent was indeed lessened compared to that in A2780 cells when cisplatin was administered at 2, 4, 8 or 16 μg/ml. Consistent with the above results, Cx32 knockdown in A2780 cells partially abrogated the cisplatin resistance induced by USP14 silencing (Fig. 4C). These findings suggest that Cx32 plays an important role in USP14 inhibition-induced cisplatin resistance.

Inhibition of USP14 induces Cx32 internalization and impairs GJIC. The upregulation of Cx32 induced by USP14 inhibition was found to contribute to cisplatin insensitivity. We aimed to ascertain whether GJIC and Cx32 localization are affected

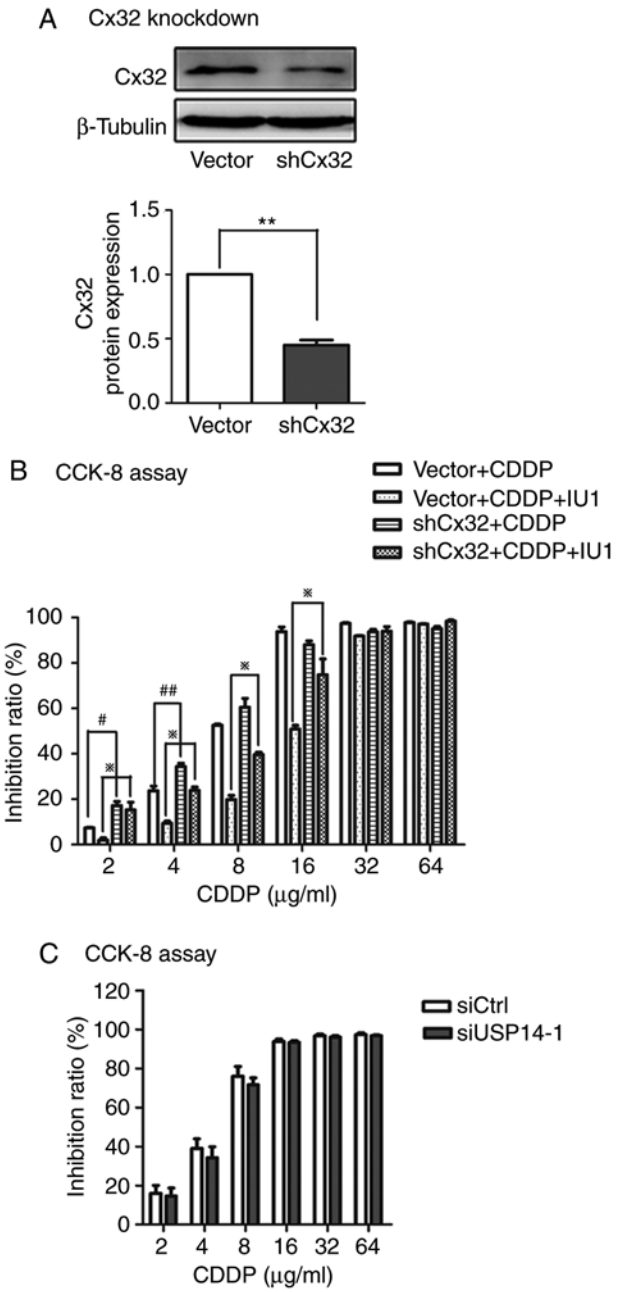

Figure 4. Cx32 knockdown counteracts USP14 inhibition-induced cisplatin resistance in A2780 cells. (A) Western blotting verified that Cx32 expression was significantly knocked down. **P<0.01. (B) Cx32 knockdown significantly increased cisplatin cytotoxicity at cisplatin (CDDP) concentrations of 2 and 4 μg/ml. Cotreatment of A2780-shCx32 cells with IU1 (50 μM, 4 h) and CDDP (8 μg/ml) impaired the anti-apoptotic effect of IU1 (50 μM, 48 h), as shown by a CCK-8 assay. (C) The anti-apoptotic effect was abolished when USP14 was knocked down in A2780-shCx32 cells. The results are presented as the mean ± SE. **P<0.01; #P<0.05; ##P<0.01; ×P<0.001. n=3. USP14, ubiquitin-specific protease 14; Cx32, connexin 32.

by USP14 inhibition. As depicted in Fig. 1A, USP14 suppression caused a marked reduction in GJIC (Fig. 5A). In addition, membrane and cytoplasmic proteins were extracted after administration of IU1 or siUSP14-1. As expected, the results demonstrated that Cx32 was predominantly distributed in the cytoplasm and the Cx32 that localized on the membrane was decreased (Fig. 5B and C). In summary, Cx32 internalization caused by USP14 inhibition caused the cisplatin insensitivity in a non-gap junction-mediated manner.

Discussion

The results of the present study indicated that decreased expression and activity of USP14 in A2780-CDDP cells resulted in upregulation and internalization of Cx32, which contributed to cisplatin resistance.

Previous studies have reported that expression and activity of USP14 are elevated in gastric carcinoma, ovarian cancer and melanoma. Knockdown of this 19S proteasome-associated DUB sensitizes cancer to chemotherapeutics and induces apoptosis (25,26,50). To the best of ou knowledge, this evidence is the first to show that the expression and activity of USP14 are downregulated in A2780-CDDP cells and that the reduction in the expression and activity of USP14 is associated with cisplatin insensitivity. These findings suggest that USP14 is not only a target of oncotherapy but also a marker of chemoresistance.

Studies indicate that the cytoplasmic localization of Cx32 serves as a pro-tumor factor in a number of cancer types (11,14). Similarly, in the present study, it was shown that the internalization of Cx32 and reduction in GJIC induced by USP14 inhibition contributed to cisplatin resistance. This effect is not limited to Cx32. Cx26 was found to be cytoplasmic in human invasive carcinomas of the breast (51). Intracellular accumulation of Cx43 and Cx32 was observed in human prostate cancer cells and facilitated their malignant phenotype (52). Furthermore, it is important to note that even nuclear localization of Cx32 has been reported and suppresses streptonigrin/cisplatin-induced apoptosis (13). Taken together, these findings indicate that the upregulation and mis-localization of Cx play a pro-tumor role in a non-junctional manner.

Regarding the reasons for the augmentation of Cx32 protein expression by USP14 inhibition, the qPCR results demonstrated that the Cx32 mRNA level remained unchanged, indicating that the increase in Cx32 protein expression was not due to an upregulated transcription level. Toler *et al* noted that mRNA of Cx was detected without corresponding levels in Cx protein expression (53). In this study, posttranslational modifications may be responsible for the increased expression and cytoplasmic localization of Cx32 based on the fact that USP14 is a DUB modulating ubiquitination and degradation. The E3 ubiquitin ligase, AMSH (associated molecule with the SH3 domain of STAM) and a number of ubiquitin-binding proteins such as EGF receptor pathway substrate 15 (Eps15), hepatocyte growth factor-regulated tyrosine kinase substrate (Hrs) and tumor susceptibility gene 101 (TSG101) were implicated in modulating Cx43 localization and GJIC (20,54-56). Cx26 and Cx32 have also been shown to undergo ubiquitination (57,58). However, in this study, the ubiquitination level of Cx32 remained unchanged when USP14 was inhibited, suggesting that Cx32 was not directly affected by USP14. It has been reported that Wnt signaling (59), NF-κB signaling (60) and the estrogen receptor (ER) signaling pathway (24) are mediated by USP14. Furthermore, Xu *et al* reported that USP14 regulates autophagy by suppressing K63 ubiquitination of Beclin 1 (61). Cx32 may be regulated by USP14 inhibition via the signaling pathways mentioned above.

As for the mechanism of cisplatin resistance by USP14 inhibition, we demonstrated that Cx32 knockdown partially decreased the cisplatin resistance induced by USP14 inhibition. Although Cx32 upregulation by USP14 inhibition was found to be an important factor to counteract cisplatin cytotoxicity,

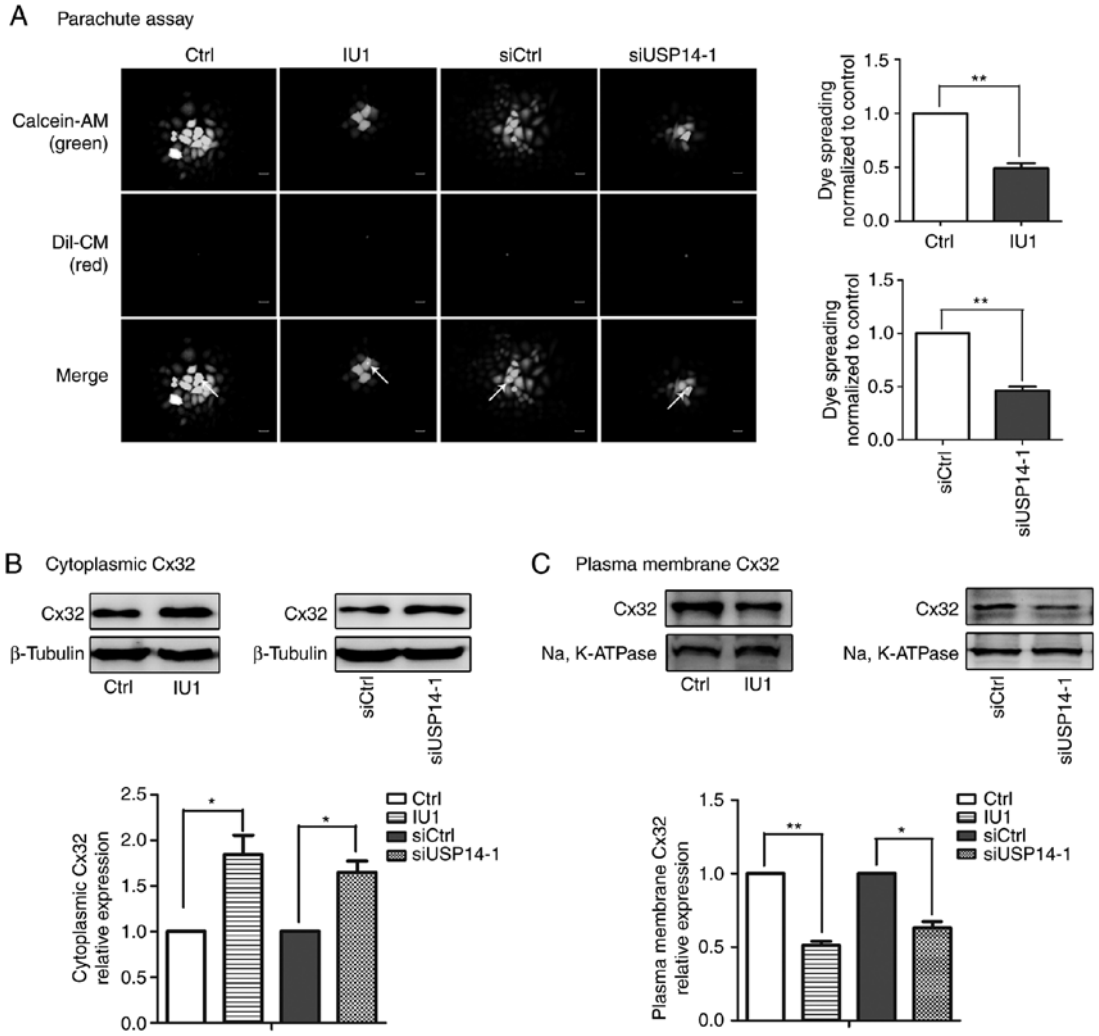

Figure 5. USP14 inhibition promotes Cx32 internalization and impaired GJIC. (A) Relative to the control treatment, both 50 μM IU1 and siUSP14-1 decreased GJIC. The cells were dyed green with Calcein-AM and dyed red with Dil-CM. In merged figures, the arrows indicate donor cells that were dyed red and green and the rest of the cells were green-stained receptor cells. The average number of receiver cells (green fluorescence) around every donor cell (both green and red fluorescence) was recorded as an index of GJIC. (B) Inhibition of USP14 increased Cx32 expression in the cytoplasm. (C) Inhibition of USP14 reduced Cx32 protein expression on the plasma membrane. The results are presented as the mean ± SE. Scale bar, 20 μm. *P<0.05 and **P<0.01. n=3. Ctrl, control; USP14, ubiquitin-specific protease 14; Cx32, connexin 32; GJIC, gap junction intercellular communication.

there still may exist other mechanisms. Lee *et al* showed that inhibition of USP14 by IU1 enhanced the proteasome activity and accelerated the degradation of oxidized proteins (22). Sharma *et al* reported that USP14 inhibition stabilized RNF168 and restored downstream DNA damage response (DDR) signaling, thus protecting prostate cancer cells from radiotherapy (62). Furthermore, USP14 was found to modulate hippocampal short-term plasticity and long-term memory formation independent of its deubiquitinating activity (63,64). In the present study, eliminating toxic proteins, facilitating DNA repair and other signaling pathways regulated by USP14 may also have accounted for the observed cisplatin insensitivity. Although many studies have demonstrated the importance of USP14 in cell physiology and diseases, the global substrates of USP14 are still to be elucidated, representing a major 'bottleneck' to uncover the functional characterization of USP14 and understand the complexity of proteasome-associated deubiquitination events (65,66).

The tumor-promoting effect of USP14 inhibition is strongly supported by *in vitro* data, but only one cell line was used in this research, thus, this may be a limitation of this study and further investigation using more cell lines to determine the underlying mechanism of USP14 is warranted in the future. Moreover, clinical pathology and *in vivo* experiments are needed for definite confirmation. Our experimental results support the hypothesis that USP14 inhibition results in the abnormal distribution of Cx32 and the dysfunction of GJIC, while Cx32 is not a direct target of USP14, and the mechanism underlying Cx32 internalization requires further study.

In conclusion, the expression and activity of USP14 were markedly decreased, accompanied by cisplatin resistance, in A2780-CDDP cells. USP14 inhibition led to the upregulation and internalization of Cx32 and the impairment of GJIC, which mediates cisplatin resistance in A2780 cells. Recovering the mechanism of Cx32 internalization and trafficking may be a potential therapy against tumors and chemoresistance.

Acknowledgements

Not applicable.

Funding

This study was funded by the National Natural Science Foundation of China (grant no. 81473234), the Joint Fund of the National Natural Science Foundation of China (grant no. U1303221), the Fundamental Research Funds for the Central Universities (grant no. 16ykjc01) and a grant from the Department of Science and Technology of Guangdong Province (grant no. 20160908).

Availability of data and materials

The datasets used and/or analyzed during the present study are available from the corresponding author on reasonable request.

Authors' contributions

LT, QW and GH conceived and designed the study. HL, XW performed the siRNA and shRNA transfection experiments, CCK-8 assay and western blot. NZ performed the flow cytometry experiments, collected and analyse the data. YF was involved in cell culture and parachute dye-coupling assay. FP made substantial contributions in the acquisition and interpretation of the data. HL and HG wrote the manuscript. LT and XW revised and amended the draft. QW contributed to final approval of the version to be published. All authors read and approved the final manuscript and agree to be accountable for all aspects of the research in ensuring that the accuracy or integrity of any part of the work are appropriately investigated and resolved.

Ethics approval and consent to participate

Not applicable.

Patient consent for publication

Not applicable.

Competing interests

The authors declare that they have no competing interests.

References

1. Mikula-Pietrasik J, Witucka A, Pakula M, Uruski P, Begier-Krasińska B, Niklas A, Tykarski A and Książek K: Comprehensive review on how platinum- and taxane-based chemotherapy of ovarian cancer affects biology of normal cells. Cell Mol Life Sci 76: 681-697, 2019.
2. Norouzi-Barough L, Sarookhani MR, Sharifi M, Moghbelinejad S, Jangjoo S and Salehi R: Molecular mechanisms of drug resistance in ovarian cancer. J Cell Physiol 233: 4546-4562, 2018.
3. Kujawa KA and Lisowska KM: Ovarian cancer-from biology to clinic. Postepy Hig Med Dosw (Online) 2: 1275-1290, 2015 (In Polish).
4. Aasen T, Mesnil M, Naus CC, Lampe PD and Laird DW: Gap junctions and cancer: Communicating for 50 years. Nat Rev Cancer 16: 775-788, 2016.
5. Ruch RJ: Connexin43 suppresses lung cancer stem cells. Cancers (Basel) 11: pii: E175, 2019.
6. Suzhi Z, Liang T, Yuexia P, Lucy L, Xiaoting H, Yuan Z and Qin W: Gap junctions enhance the antiproliferative effect of MicroRNA-124-3p in glioblastoma cells. J Cell Physiol 230: 2476-2488, 2015.
7. Polusani SR, Kalmykov EA, Chandrasekhar A, Zucker SN and Nicholson BJ: Cell coupling mediated by connexin 26 selectively contributes to reduced adhesivity and increased migration. J Cell Sci 129: 4399-4410, 2016.
8. Chen Q, Boire A, Jin X, Valiente M, Er EE, Lopez-Soto A, Jacob L, Patwa R, Shah H, Xu K, *et al*: Carcinoma-astrocyte gap junctions promote brain metastasis by cGAMP transfer. Nature 533: 493-498, 2016.
9. Kawasaki Y, Omori Y, Li Q, Nishikawa Y, Yoshioka T, Yoshida M, Ishikawa K and Enomoto K: Cytoplasmic accumulation of connexin32 expands cancer stem cell population in human HuH7 hepatoma cells by enhancing its self-renewal. Int J Cancer 128: 51-62, 2011.
10. Li Q, Omori Y, Nishikawa Y, Yoshioka T, Yamamoto Y and Enomoto K: Cytoplasmic accumulation of connexin32 protein enhances motility and metastatic ability of human hepatoma cells in vitro and in vivo. Int J Cancer 121: 536-546, 2007.
11. Wu W, Fan L, Bao Z, Zhang Y, Peng Y, Shao M, Xiang Y, Zhang X, Wang Q and Tao L: The cytoplasmic translocation of Cx32 mediates cisplatin resistance in ovarian cancer cells. Biochem Biophys Res Commun 487: 292-299, 2017.
12. Zhang Y, Tao L, Fan LX, Huang K, Luo HM, Ge H, Wang X and Wang Q: Cx32 mediates cisplatin resistance in human ovarian cancer cells by affecting drug efflux transporter expression and activating the EGFR-Akt pathway. Mol Med Rep 19: 2287-2296, 2019.
13. Zhao Y, Lai Y, Ge H, Guo Y, Feng X, Song J, Wang Q, Fan L, Peng Y, Cao M, *et al*: Non-junctional Cx32 mediates anti-apoptotic and pro-tumor effects via epidermal growth factor receptor in human cervical cancer cells. Cell Death Dis 8: e2773, 2017.
14. Xiang Y, Wang Q, Guo Y, Ge H, Fu Y, Wang X and Tao L: Cx32 exerts anti-apoptotic and pro-tumor effects via the epidermal growth factor receptor pathway in hepatocellular carcinoma. J Exp Clin Cancer Res 38: 145, 2019.
15. Saeki Y: Ubiquitin recognition by the proteasome. J Biochem 161: 113-124, 2017.
16. Kwon YT and Ciechanover A: The ubiquitin code in the ubiquitin-proteasome system and autophagy. Trends Biochem Sci 42: 873-886, 2017.
17. Salat-Canela C, Munoz MJ, Sese M, Ramon y Cajal S and Aasen T: Post-transcriptional regulation of connexins. Biochem Soc Trans 43: 465-470, 2015.
18. Aasen T, Johnstone S, Vidal-Brime L, Lynn KS and Koval M: Connexins: Synthesis, Post-translational modifications, and trafficking in health and disease. Int J Mol Sci 19: pii: E1296, 2018.
19. Spagnol G, Kieken F, Kopanic JL, Li H, Zach S, Stauch KL, Grosely R and Sorgen PL: Structural studies of the Nedd4 WW domains and their selectivity for the Connexin43 (Cx43) Carboxyl terminus. J Biol Chem 291: 7637-7650, 2016.
20. Totland MZ, Bergsland CH, Fykerud TA, Knudsen LM, Rasmussen NL, Eide PW, Yohannes Z, Sørensen V, Brech A, Lothe RA and Leithe E: The E3 ubiquitin ligase NEDD4 induces endocytosis and lysosomal sorting of connexin 43 to promote loss of gap junctions. J Cell Sci 130: 2867-2882, 2017.
21. Sun J, Hu Q, Peng H, Peng C, Zhou L, Lu J and Huang C: The ubiquitin-specific protease USP8 deubiquitinates and stabilizes Cx43. J Biol Chem 293: 8275-8284, 2018.
22. Lee BH, Lee MJ, Park S, Oh DC, Elsasser S, Chen PC, Gartner C, Dimova N, Hanna J, Gygi SP, *et al*: Enhancement of proteasome activity by a small-molecule inhibitor of USP14. Nature 467: 179-184, 2010.
23. Chen X, Yang Q, Chen J, Zhang P, Huang Q, Zhang X, Yang L, Xu D, Zhao C, Wang X and Liu J: Inhibition of proteasomal deubiquitinase by silver complex induces apoptosis in non-small cell lung cancer cells. Cell Physiol Biochem 49: 780-797, 2018.
24. Xia X, Liao Y, Guo Z, Li Y, Jiang L, Zhang F, Huang C, Liu Y, Wang X, Liu N, *et al*: Targeting proteasome-associated deubiquitinases as a novel strategy for the treatment of estrogen receptor-positive breast cancer. Oncogenesis 7: 75, 2018.
25. Wang Y, Wang J, Zhong J, Deng Y, Xi Q, He S, Yang S, Jiang L, Huang M, Tang C and Liu R: Ubiquitin-specific protease 14 (USP14) regulates cellular proliferation and apoptosis in epithelial ovarian cancer. Med Oncol 32: 379, 2015.
26. Fu Y, Ma G, Liu G, Li B, Li H, Hao X and Liu L: USP14 as a novel prognostic marker promotes cisplatin resistance via Akt/ERK signaling pathways in gastric cancer. Cancer Med 7: 5577-5588, 2018.
27. Hu X, Meng Y, Xu L, Qiu L, Wei M, Su D, Qi X, Wang Z, Yang S, Liu C and Han J: Cul4 E3 ubiquitin ligase regulates ovarian cancer drug resistance by targeting the antiapoptotic protein BIRC3. Cell Death Dis 10: 104, 2019.

28. Lu Y, Han D, Liu W, Huang R, Ou J, Chen X, Zhang X, Wang X, Li S, Wang L, *et al*: RNF138 confers cisplatin resistance in gastric cancer cells via activating Chk1 signaling pathway. Cancer Biol Ther 19: 1128-1138, 2018.
29. Li L, Liu T, Li Y, Wu C, Luo K, Yin Y, Chen Y, Nowsheen S, Wu J, Lou Z and Yuan J: The deubiquitinase USP9X promotes tumor cell survival and confers chemoresistance through YAP1 stabilization. Oncogene 37: 2422-2431, 2018.
30. Denkert C, Budczies J, Darb-Esfahani S, Györffy B, Sehouli J, Könsgen D, Zeillinger R, Weichert W, Noske A, Buckendahl AC, *et al*: A prognostic gene expression index in ovarian cancer-validation across different independent data sets. J Pathol 218: 273-280, 2009.
31. Ahmed AA, Mills AD, Ibrahim AE, Temple J, Blenkiron C, Vias M, Massie CE, Iyer NG, McGeoch A, Crawford R, *et al*: The extracellular matrix protein TGFBI induces microtubule stabilization and sensitizes ovarian cancers to paclitaxel. Cancer Cell 12: 514-527, 2007.
32. Mok SC, Bonome T, Vathipadiekal V, Bell A, Johnson ME, Wong KK, Park DC, Hao K, Yip DK, Donninger H, *et al*: A gene signature predictive for outcome in advanced ovarian cancer identifies a survival factor: Microfibril-associated glycoprotein 2. Cancer Cell 16: 521-532, 2009.
33. Konstantinopoulos PA, Spentzos D, Karlan BY, Taniguchi T, Fountzilas E, Francoeur N, Levine DA and Cannistra SA: Gene expression profile of BRCAness that correlates with responsiveness to chemotherapy and with outcome in patients with epithelial ovarian cancer. J Clin Oncol 28: 3555-3561, 2010.
34. Marchion DC, Cottrill HM, Xiong Y, Chen N, Bicaku E, Fulp WJ, Bansal N, Chon HS, Stickles XB, Kamath SG, *et al*: BAD phosphorylation determines ovarian cancer chemosensitivity and patient survival. Clin Cancer Res 17: 6356-6366, 2011.
35. Mateescu B, Batista L, Cardon M, Gruosso T, de Feraudy Y, Mariani O, Nicolas A, Meyniel JP, Cottu P, Sastre-Garau X and Mechta-Grigoriou F: miR-141 and miR-200a act on ovarian tumorigenesis by controlling oxidative stress response. Nat Med 17: 1627-1635, 2011.
36. Gentric G, Kieffer Y, Mieulet V, Goundiam O, Bonneau C, Nemati F, Hurbain I, Raposo G, Popova T, Stern MH, *et al*: PML-regulated mitochondrial metabolism enhances chemosensitivity in human ovarian cancers. Cell Metab 29: 156-173.e110, 2019.
37. Bonome T, Levine DA, Shih J, Randonovich M, Pise-Masison CA, Bogomolniy F, Ozbun L, Brady J, Barrett JC, Boyd J and Birrer MJ: A gene signature predicting for survival in suboptimally debulked patients with ovarian cancer. Cancer Res 68: 5478-5486, 2008.
38. Vathipadiekal V, Wang V, Wei W, Waldron L, Drapkin R, Gillette M, Skates S and Birrer M: Creation of a human secretome: A novel composite library of human secreted proteins: Validation using ovarian cancer gene expression data and a virtual secretome array. Clin Cancer Res 21: 4960-4969, 2015.
39. King ER, Tung CS, Tsang YT, Zu Z, Lok GT, Deavers MT, Malpica A, Wolf JK, Lu KH, Birrer MJ, *et al*: The anterior gradient homolog 3 (AGR3) gene is associated with differentiation and survival in ovarian cancer. Am J Surg Pathol 35: 904-912, 2011.
40. Ferriss JS, Kim Y, Duska L, Birrer M, Levine DA, Moskaluk C, Theodorescu D and Lee JK: Multi-gene expression predictors of single drug responses to adjuvant chemotherapy in ovarian carcinoma: Predicting platinum resistance. PLoS One 7: e30550, 2012.
41. Bild AH, Yao G, Chang JT, Wang Q, Potti A, Chasse D, Joshi MB, Harpole D, Lancaster JM, Berchuck A, *et al*: Oncogenic pathway signatures in human cancers as a guide to targeted therapies. Nature 439: 353-357, 2006.
42. Koti M, Gooding RJ, Nuin P, Haslehurst A, Crane C, Weberpals J, Childs T, Bryson P, Dharsee M, Evans K, *et al*: Identification of the IGF1/PI3K/NF κB/ERK gene signalling networks associated with chemotherapy resistance and treatment response in high-grade serous epithelial ovarian cancer. BMC Cancer 13: 549, 2013.
43. Lisowska KM, Olbryt M, Dudaladava V, Pamuła-Piłat J, Kujawa K, Grzybowska E, Jarząb M, Student S, Rzepecka IK, Jarząb B and Kupryjańczyk J: Gene expression analysis in ovarian cancer-faults and hints from DNA microarray study. Front Oncol 4: 6, 2014.
44. Uehara Y, Oda K, Ikeda Y, Koso T, Tsuji S, Yamamoto S, Asada K, Sone K, Kurikawa R, Makii C, *et al*: Integrated copy number and expression analysis identifies profiles of whole-arm chromosomal alterations and subgroups with favorable outcome in ovarian clear cell carcinomas. PLoS One 10: e0128066, 2015.
45. Tothill RW, Tinker AV, George J, Brown R, Fox SB, Lade S, Johnson DS, Trivett MK, Etemadmoghadam D, Locandro B, *et al*: Novel molecular subtypes of serous and endometrioid ovarian cancer linked to clinical outcome. Clin Cancer Res 14: 5198-5208, 2008.
46. Zhao C, Chen X, Zang D, Lan X, Liao S, Yang C, Zhang P, Wu J, Li X, Liu N, *et al*: Platinum-containing compound platinum pyrithione is stronger and safer than cisplatin in cancer therapy. Biochem Pharmacol 116: 22-38, 2016.
47. Livak KJ and Schmittgen TD: Analysis of relative gene expression data using real-time quantitative PCR and the 2(-Delta Delta C(T)) method. Methods 25: 402-408, 2001.
48. Goldberg GS, Bechberger JF and Naus CC: A pre-loading method of evaluating gap junctional communication by fluorescent dye transfer. Biotechniques 3: 490-497, 1995.
49. Koreen IV, Elsayed WA, Liu YJ and Harris AL: Tetracycline-regulated expression enables purification and functional analysis of recombinant connexin channels from mammalian cells. Biochem J 383: 111-119, 2004.
50. Didier R, Mallavialle A, Ben Jouira R, Domdom MA, Tichet M, Auberger P, Luciano F, Ohanna M, Tartare-Deckert S and Deckert M: Targeting the proteasome-associated deubiquitinating enzyme USP14 impairs melanoma cell survival and overcomes resistance to MAPK-targeting therapies. Mol Cancer Ther 17: 1416-1429, 2018.
51. Jamieson S, Going JJ, D'Arcy R and George WD: Expression of gap junction proteins connexin 26 and connexin 43 in normal human breast and in breast tumours. J Pathol 184: 37-43, 1998.
52. Govindarajan R, Zhao S, Song XH, Guo RJ, Wheelock M, Johnson KR and Mehta PP: Impaired Trafficking of connexins in androgen-independent human prostate cancer cell lines and its mitigation by alpha-catenin. J Biol Chem 277: 50087-50097, 2002.
53. Toler CR, Taylor DD and Gercel-Taylor C: Loss of communication in ovarian cancer. Am J Obstet Gynecol 194: e27-e31, 2006.
54. Ribeiro-Rodrigues TM, Catarino S, Marques C, Ferreira JV, Martins-Marques T, Pereira P and Girão H: AMSH-mediated deubiquitination of Cx43 regulates internalization and degradation of gap junctions. FASEB J 28: 4629-4641, 2014.
55. Girao H, Catarino S and Pereira P: Eps15 interacts with ubiquitinated Cx43 and mediates its internalization. Exp Cell Res 315: 3587-3597, 2009.
56. Auth T, Schluter S, Urschel S, Kussmann P, Sonntag S, Höher T, Kreuzberg MM, Dobrowolski R and Willecke K: The TSG101 protein binds to connexins and is involved in connexin degradation. Exp Cell Res 315: 1053-1062, 2009.
57. Alaei SR, Abrams CK, Bulinski JC, Hertzberg EL and Freidin MM: Acetylation of C-terminal lysines modulates protein turnover and stability of Connexin-32. BMC Cell Biol 19: 22, 2018.
58. Xiao D, Chen S, Shao Q, Chen J, Bijian K, Laird DW and Alaoui-Jamali MA: Dynamin 2 interacts with connexin 26 to regulate its degradation and function in gap junction formation. Int J Biochem Cell Biol 55: 288-297, 2014.
59. Jung H, Kim BG, Han WH, Lee JH, Cho JY, Park WS, Maurice MM, Han JK, Lee MJ, Finley D and Jho EH: Deubiquitination of Dishevelled by Usp14 is required for Wnt signaling. Oncogenesis 2: e64, 2013.
60. Meng Q, Cai C, Sun T, Wang Q, Xie W, Wang R and Cui J: Reversible ubiquitination shapes NLRC5 function and modulates NF-κB activation switch. J Cell Biol 211: 1025-1040, 2015.
61. Xu D, Shan B, Sun H, Xiao J, Zhu K, Xie X, Li X, Liang W, Lu X, Qian L and Yuan J: USP14 regulates autophagy by suppressing K63 ubiquitination of Beclin 1. Genes Dev 30: 1718-1730, 2016.
62. Sharma A, Alswillah T, Singh K, Chatterjee P, Willard B, Venere M, Summers MK and Almasan A: USP14 regulates DNA damage repair by targeting RNF168-dependent ubiquitination. Autophagy 14: 1976-1990, 2018.
63. Walters BJ, Hallengren JJ, Theile CS, Ploegh HL, Wilson SM and Dobrunz LE: A catalytic independent function of the deubiquitinating enzyme USP14 regulates hippocampal synaptic short-term plasticity and vesicle number. J Physiol 592: 571-586, 2014.
64. Jarome TJ, Kwapis JL, Hallengren JJ, Wilson SM and Helmstetter FJ: The ubiquitin-specific protease 14 (USP14) is a critical regulator of long-term memory formation. Learn Mem 21: 9-13, 2013.
65. Lee BH, Lu Y, Prado MA, Shi Y, Tian G, Sun S, Elsasser S, Gygi SP, King RW and Finley D: USP14 deubiquitinates proteasome-bound substrates that are ubiquitinated at multiple sites. Nature 532: 398-401, 2016.
66. Liu B, Jiang S, Li M, Xiong X, Zhu M, Li D, Zhao L, Qian L, Zhai L, Li J, *et al*: Proteome-wide analysis of USP14 substrates revealed its role in hepatosteatosis via stabilization of FASN. Nat Commun 9: 4770, 2018.